Supplementary Fig.1 In vivo CRISPR screening predicts that MDA5 loss promotes tumor immune elimination

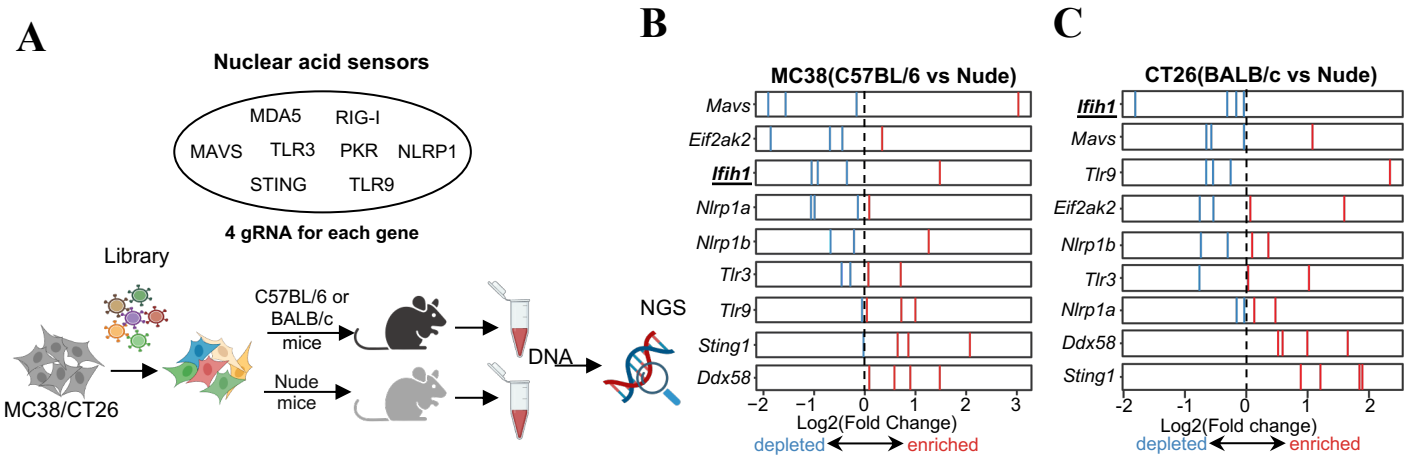

D

MC38(C57BL/6 vs Nude)

id	num	neg|score	neg|p-value
Mavs	4	0.02260	0.00000
Eif2ak2	4	0.04725	0.00000
Ifih1	4	0.06230	0.01226
Nlrp1a	4	0.06812	0.01226
Nlrp1b	4	0.23977	0.01227
Tlr3	4	0.38462	0.11171
Tlr9	4	0.84426	0.40670
Sting1	4	0.93750	0.80205
Ddx58	4	0.97505	0.98798

E

CT26(BALB/c vs Nude)

id	num	neg|score	neg|p-value
Ifih1	4	0.02375	0.06159
Mavs	4	0.04487	0.31380
Tlr9	4	0.15864	0.31381
Eif2ak2	4	0.22082	0.68857
Nlrp1b	4	0.35294	0.68857
Tlr3	4	0.39599	0.68858
Nlrp1a	4	0.52782	0.68858
Ddx58	4	0.99161	1.00000
Sting1	4	0.99609	1.00000

Supplementary Fig.2 MDA5 depletion restrains tumor growth in vivo in an immune-dependent manner

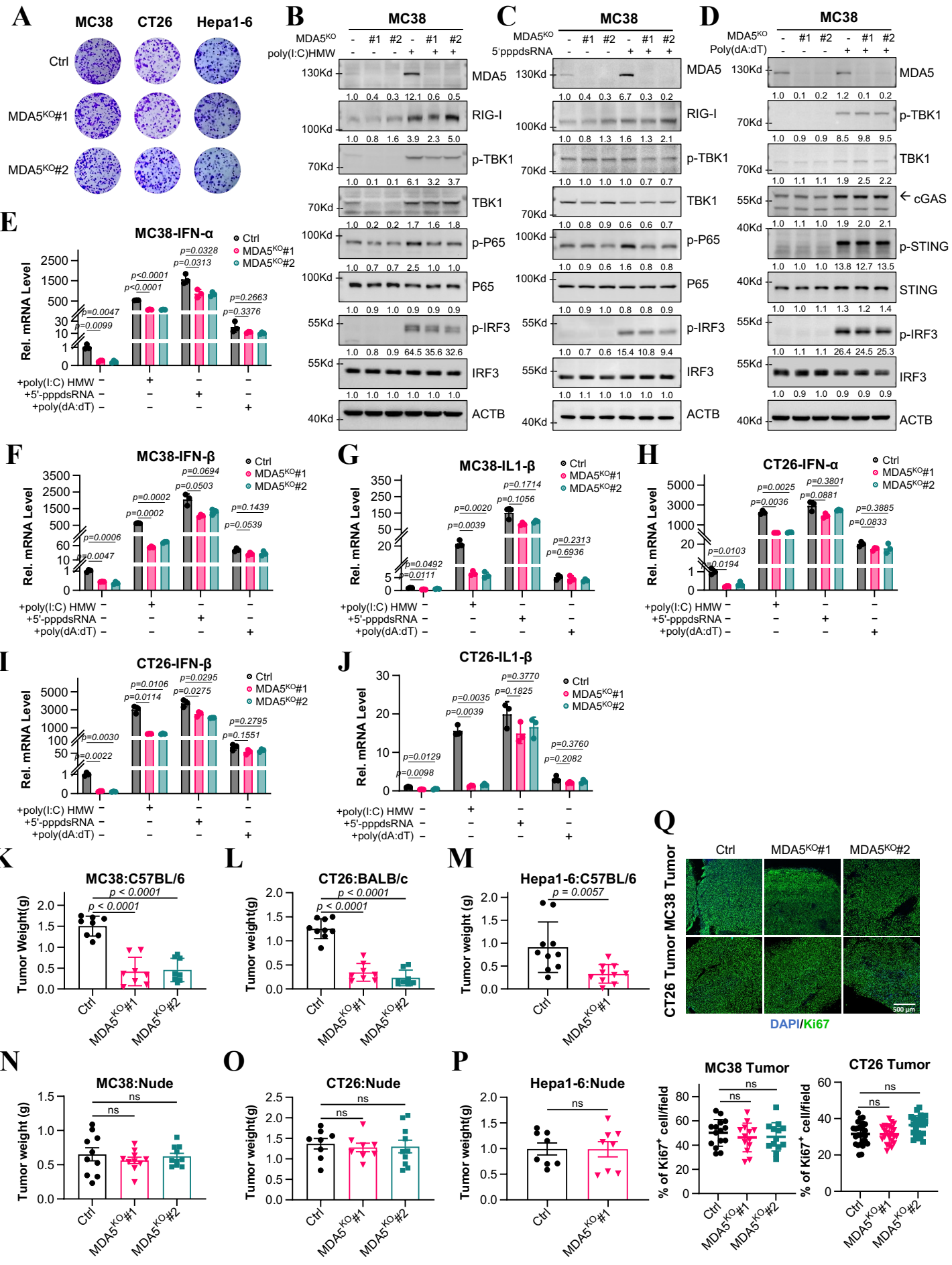

Supplementary Fig.3 MDA5 level is correlated with patient prognosis in multiple types of cancers

A

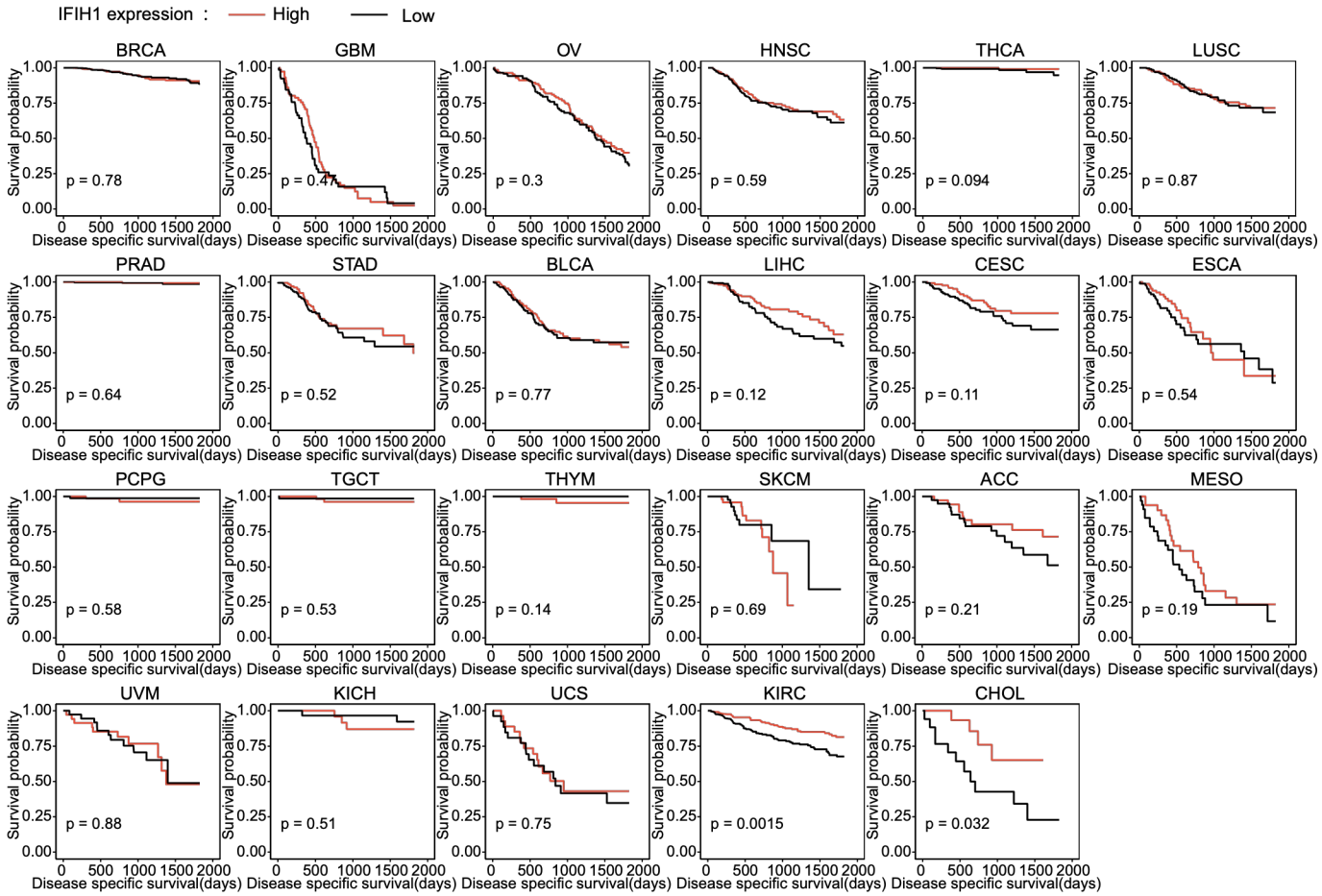

B

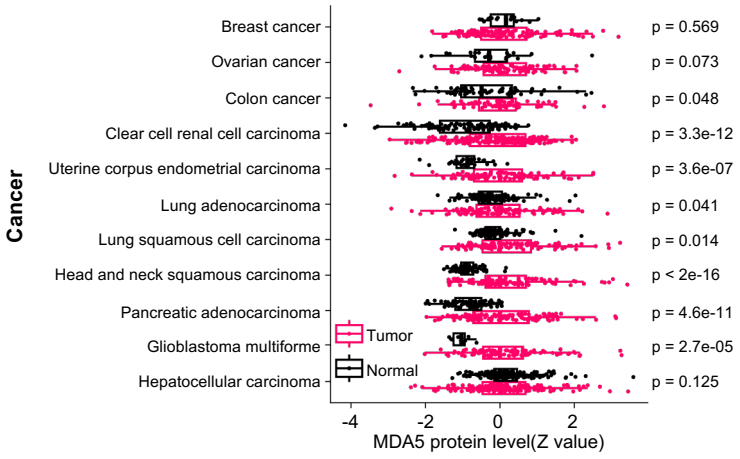

Supplementary Fig.4 MDA5 ablation remodels the tumor immune microenvironnement

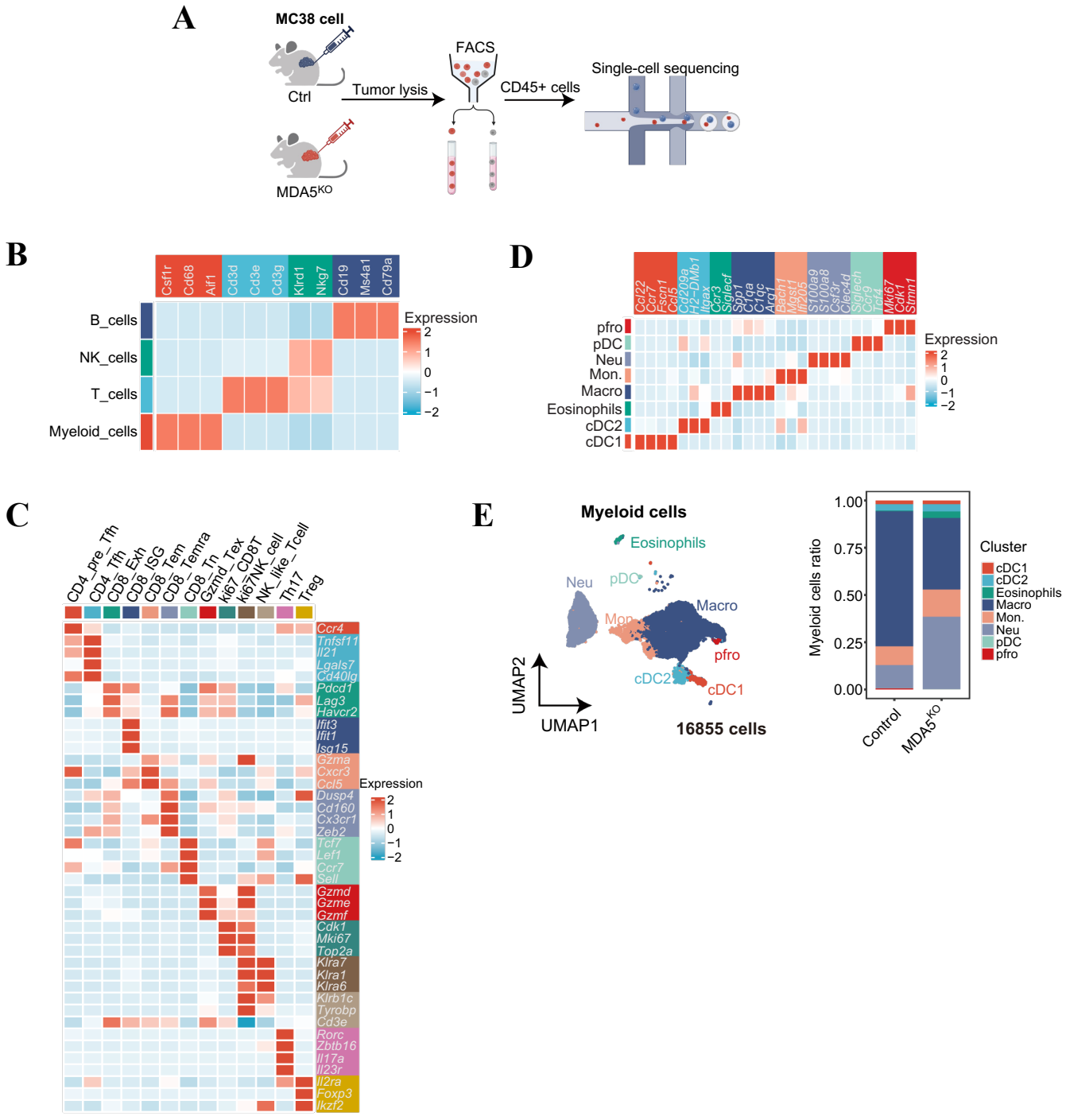

Supplementary Fig.5 MDA5-ablated tumors exhibit enhanced immune infiltration in tumor Microenvironment

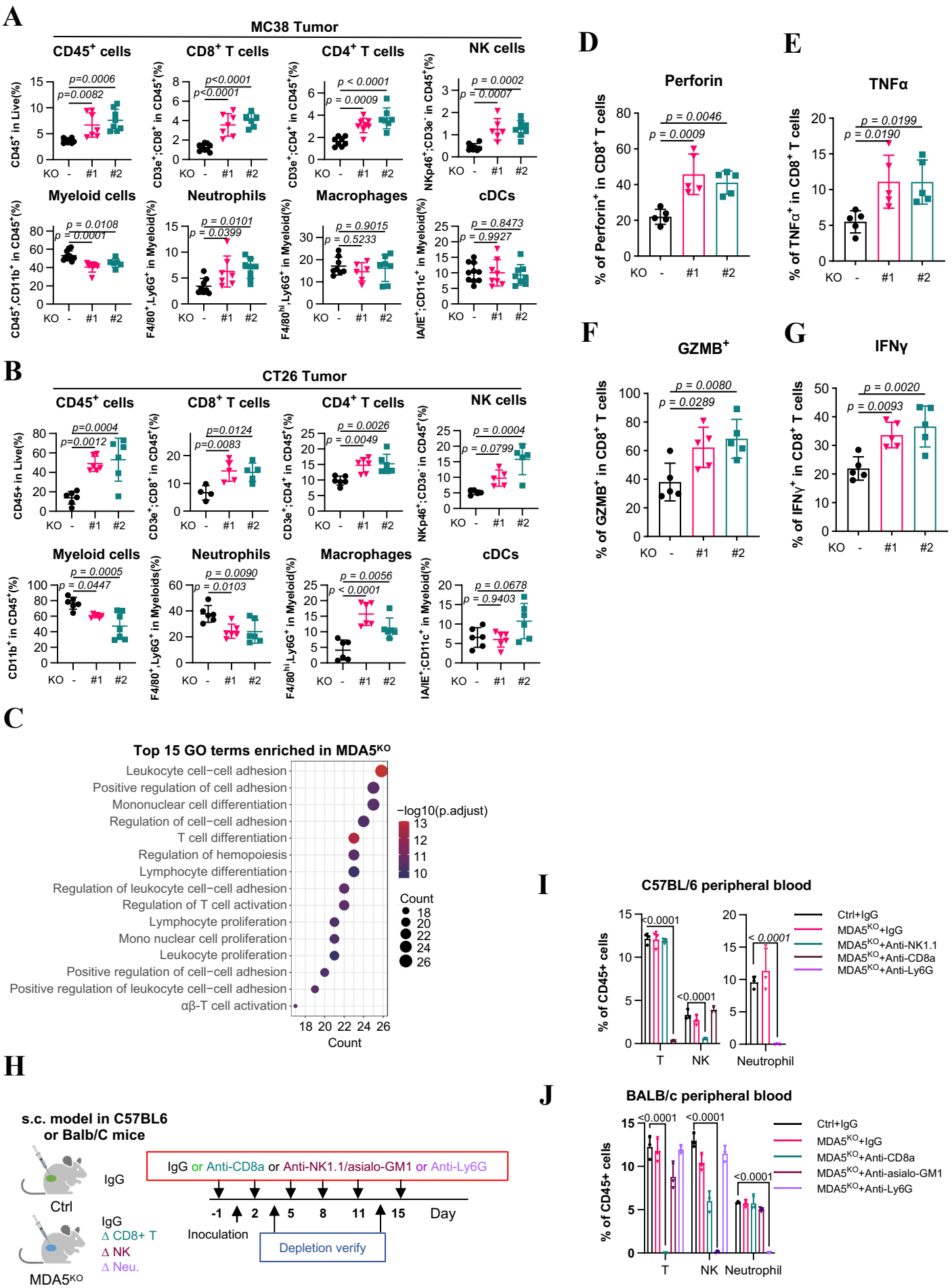

Supplementary Fig.6 MDA5-ablation promoted abscopal effect

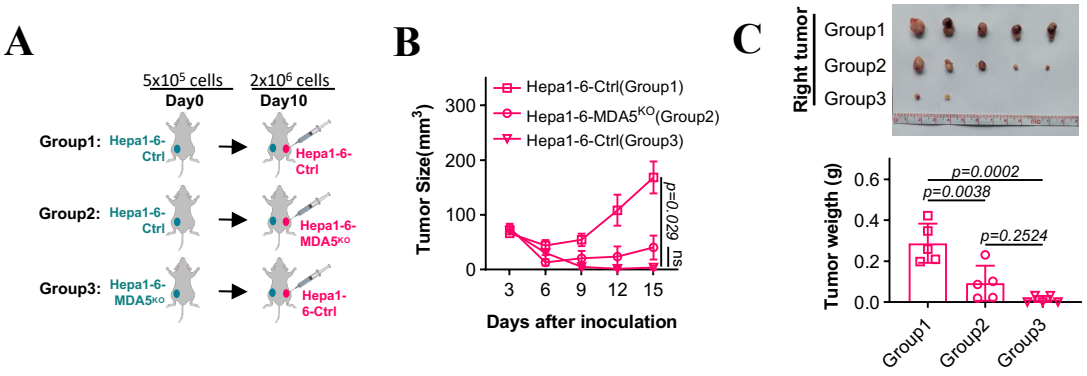

Supplementary Fig.7 MDA5-null enhances communication between CD8+T cells and DCs

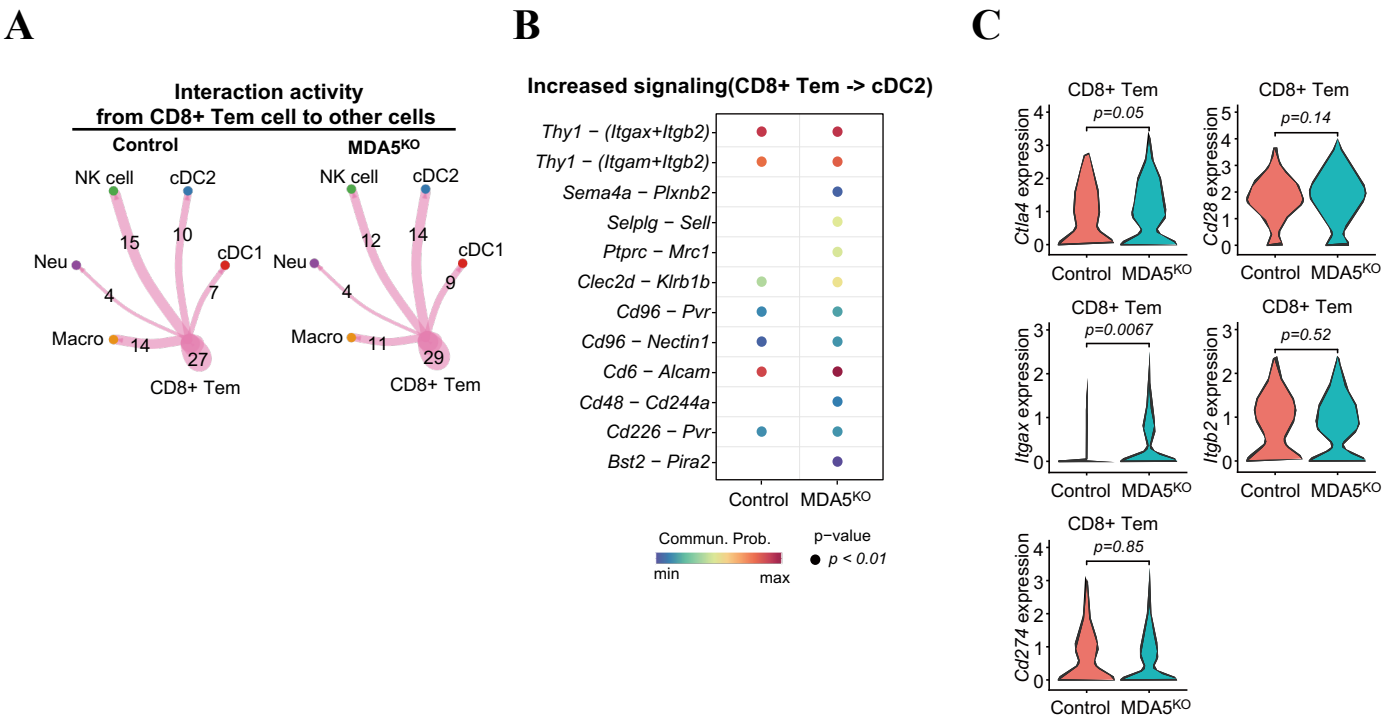

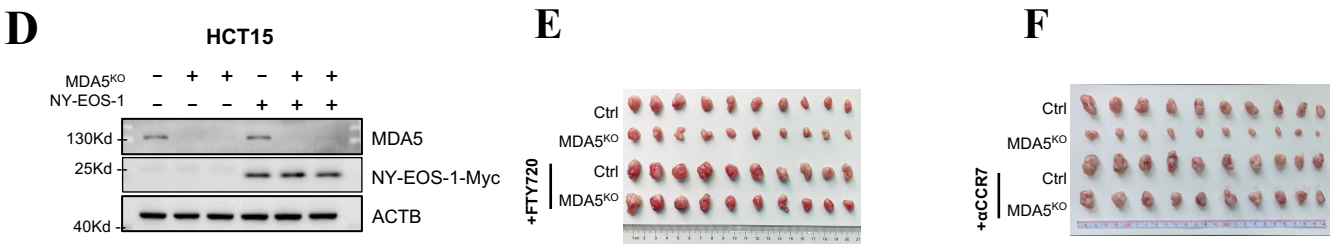

Supplementary Fig.8 MDA5 ablation promotes UPR and DAMPs expression

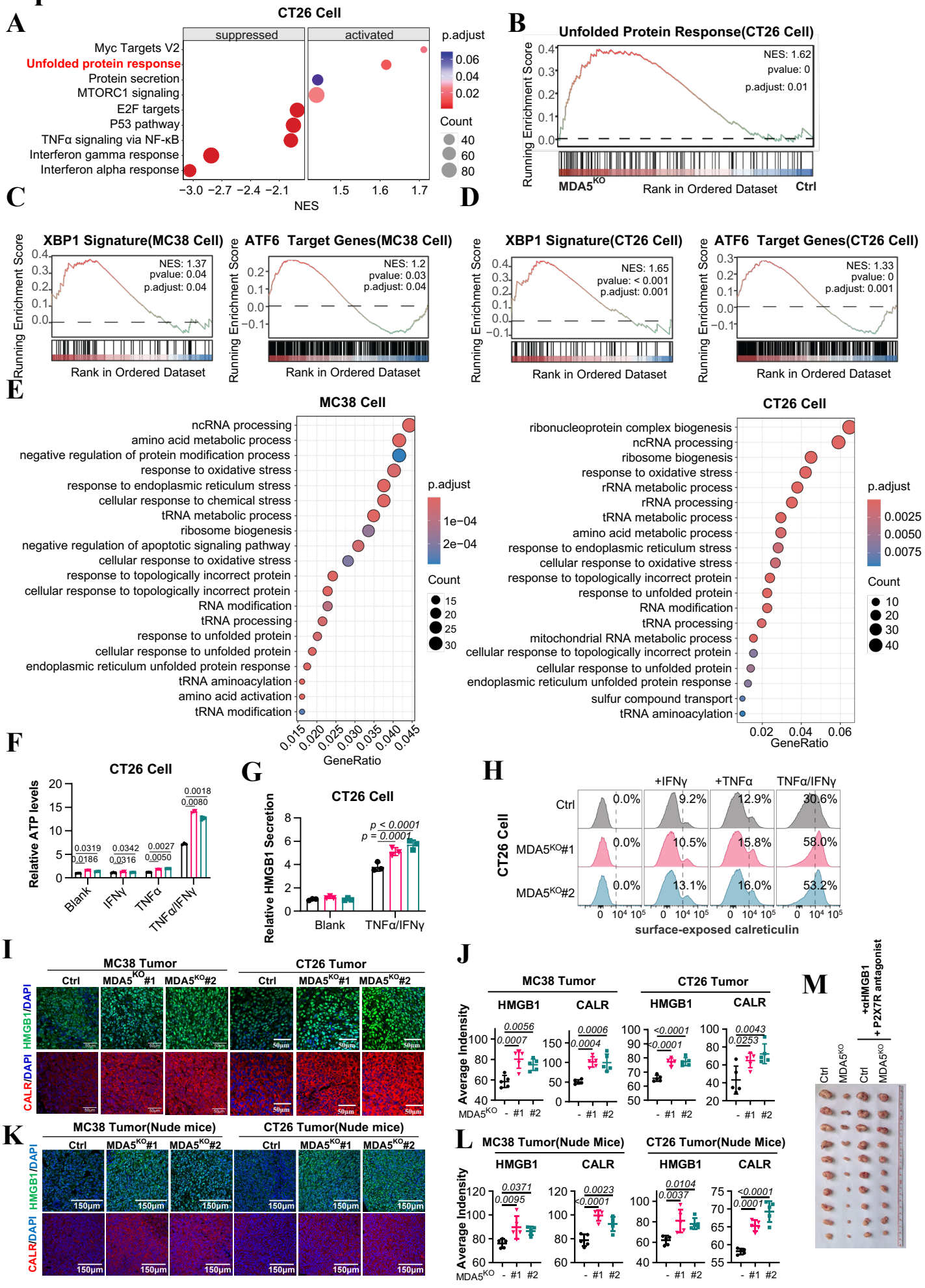

Supplementary Fig.9 DAMPs were correlated to ICD induced DC activation and T cell killing

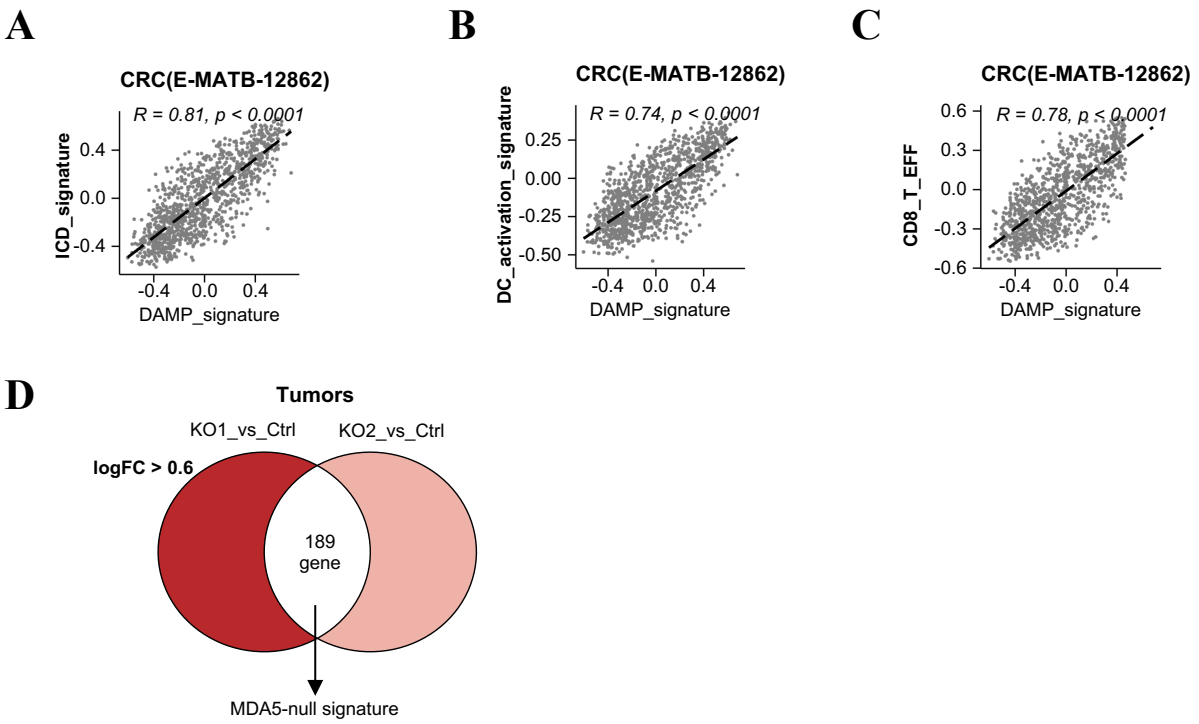

Supplementary Fig.10 MDA5 ablation sensitizes tumor cell to TNF-induced apoptosis by enhancing ASK1-JNK/P38 pathway

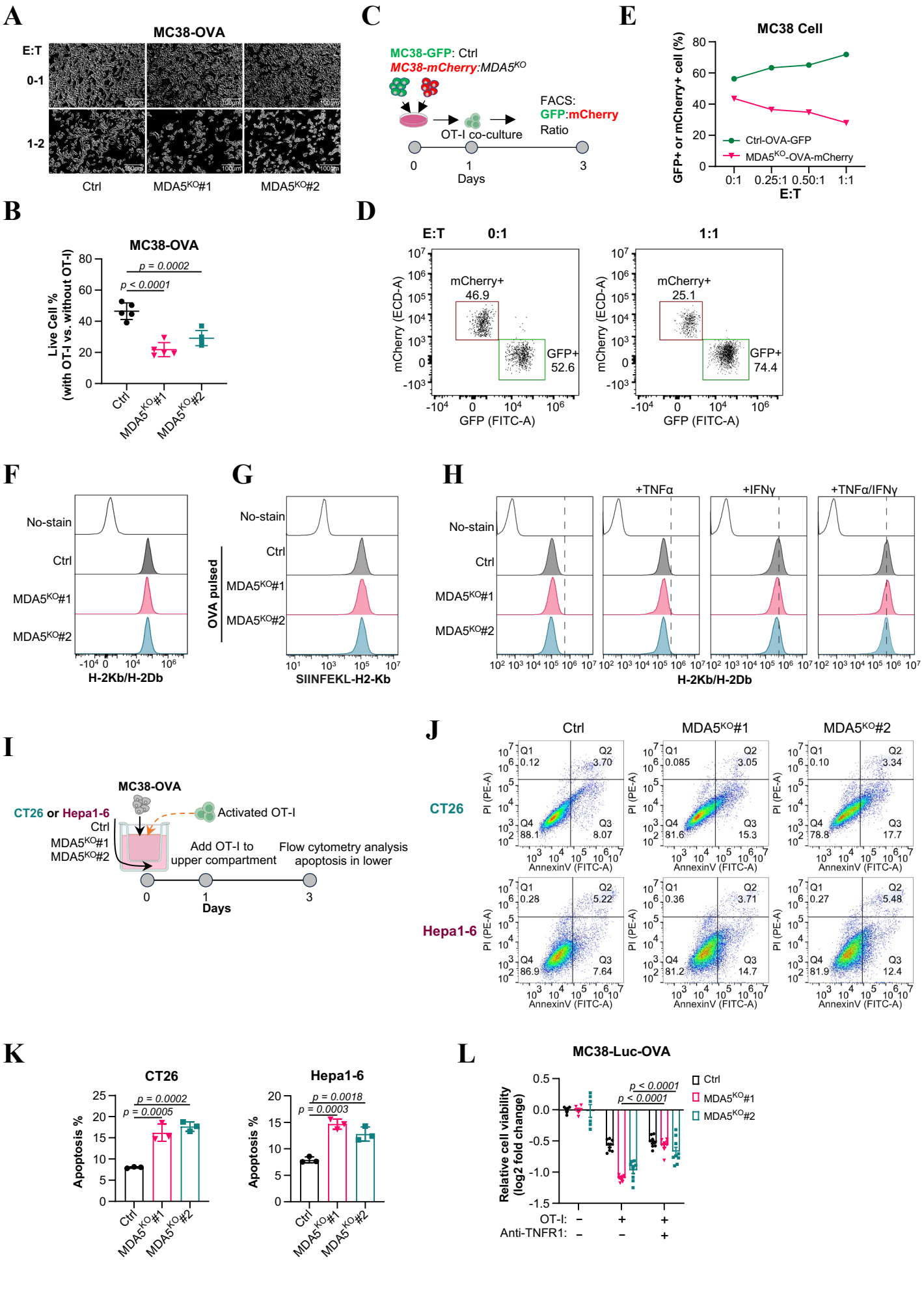

Supplementary Fig.10 MDA5 ablation sensitizes tumor cell to TNF-induced apoptosis by enhancing ASK1-JNK/P38 pathway

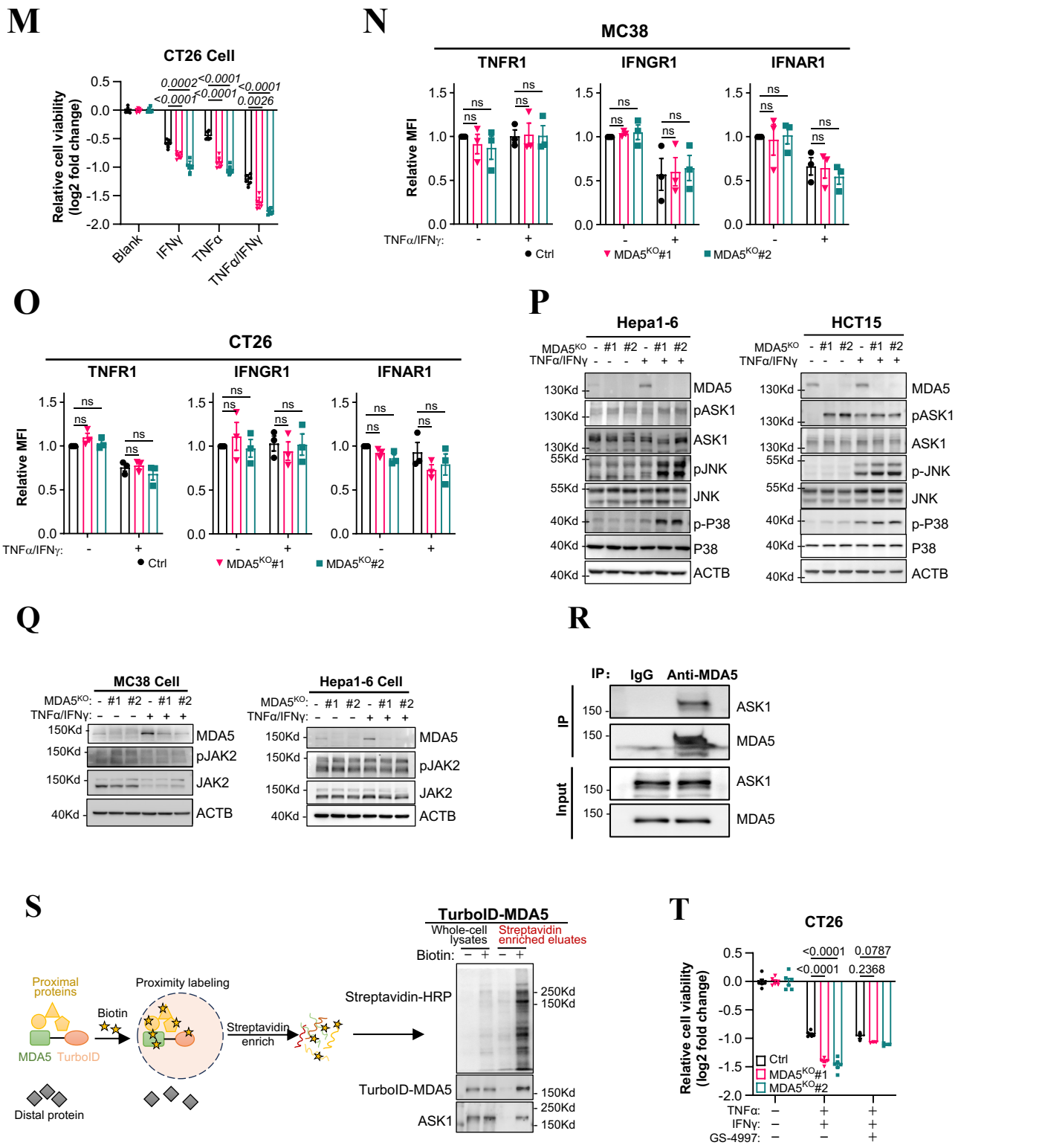

Supplementary Fig.11 MDA5-null signature predicts better response to ICB

A

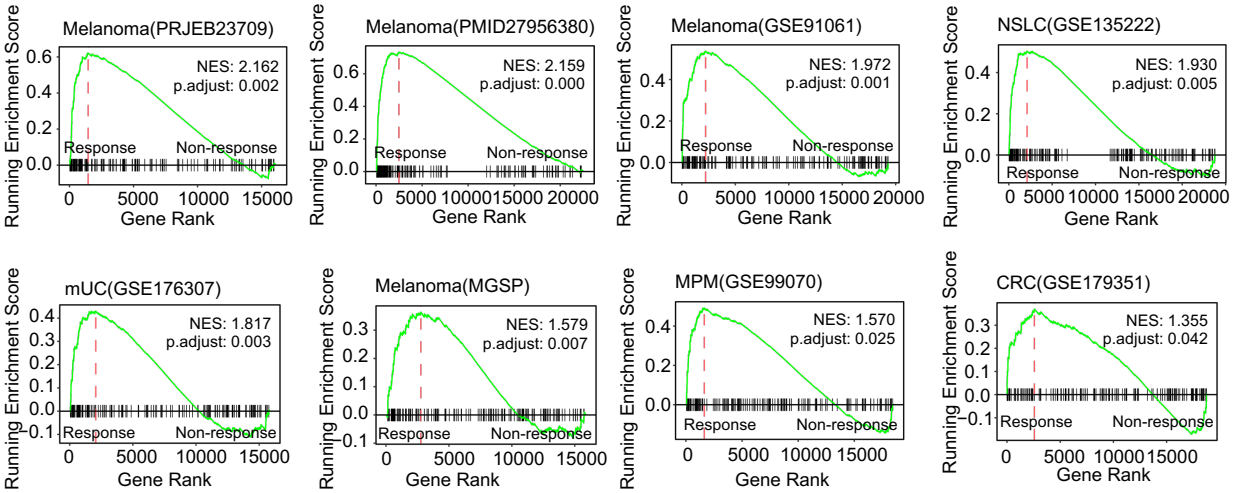

Supplementary Fig.1 In vivo CRISPR screening predicts that MDA5 loss promotes tumor immune elimination

(**A**). Schematic diagram of *in vivo* CRISPR screening targeting dsRNA sensors and related genes. (**B-C**). sgRNA rank of the enriched (red lines) and depleted (blue lines) genes in MC38(**B**) or CT26(**C**) tumors formed in immunocompetent mice compared to those in immunodeficient mice. (**D-E**). CRISPR/Cas9 screening results from MC38 (**D**) and CT26 (**E**) tumors analyzed by MAGeCK. "neg|score" corresponds to the robust ranking aggregation (RRA) lo value (0-1) of the given gene in negative selection.

Supplementary Fig. 2 | MDA5 depletion restrains tumor growth in vivo in an immune-dependent manner

(**A**)**.** Clonogenic assay of MC38, CT26, and Hepa1-6 cells following MDA5 knockout. (representative images shown). (**B-D**). Western Blot analysis of RNA sensor pathway and dsDNA sensor pathway in MC38 or MDA5-KO cells with poly(I:C) HWM(**B**), 5'-pppdsRNA (**C**) or poly(dA:dT) (**D**) treatment. Relative protein levels quantified by ImageJ are displayed under the blots after normalization to β-actin, and compared to control (first lane, set as 1.0). **(E-J)**. qRT-PCR analysis of *Ifna*, *Ifnb*, and *Il1b* mRNA expression in MC38 and CT26 cells with or without stimulation by poly(I:C) HMW, 5' ppp-dsRNA or poly(dA:dT) as indicated, relative to control cell with vehicle. (**K-M**)**.** Tumor weights of control and corresponding MDA5 knockout tumors formed in immunocompetent mice. corresponding to C-D in Figure1. (n=8-10 tumors/group. (**N-P**). Tumor weights of control and corresponding MDA5 knockout tumors formed in immunodeficient mice. corresponding to F-H in Figure1. Data are presented as the mean ± SD (n=8-10 tumors/group). (**Q**). Immunofluorescence staining and quantification of Ki67+ cells (green) in MC38 and CT26 tumors, with or without MDA5 knockout. Data are presented as mean ± SD. (n=5 tumors/group, and 3-5 fields/tumor). Statistics were applied using one-way ANOVA (**K, L, N, O, Q**), two-way ANOVA (**E-J**) or a student's t test (**M, P**).

Supplementary Fig. 3 | MDA5 level is correlated with patient prognosis in multiple types of cancers

(**A**). Kaplan–Meier survival analyses stratified by IFIH1expression levels in variant cancer types. (**B**). Analysis of MDA5 protein level across eight TCGA cancers using the CPTAC dataset. Tumor samples are coded in pink and normal samples are coded in black. Statistics were applied using rank-log test(**A**) or a student's t test (**B**).

Supplementary Fig. 4 | MDA5 ablation remodels the tumor immune microenvironnement

(**A**). Schematic representation of sample preparation for single-cell sequencing. (**B-D**). Heatmap of marker genes for each cell subpopulation. (**E**)**.** UMAP and stacked bar plots showing clusters from MC38 MDA5 knockout and the corresponding vector control tumor models. Re-clustered Myeloid cells are shown.

Supplementary Fig. 5 | MDA5-ablated tumors exhibit enhanced immune infiltration in tumor Microenvironment

(**A-B**). Quantitative estimate of various immune cells in the vector control and MDA5 knockout MC38 tumors(**A**) and CT26 tumors(**B**), as analyzed by flow cytometry. Cell populations were identified as $CD45^+$ cells ($CD45^+$), $CD8^+$ T cells ($CD45^+$,$CD3e^+$,$CD8a^+$), $CD4^+$ T cells ($CD45^+$,$CD3e^+$,$CD4^+$), NK cells ($CD45^+$,$CD3e^-$,$Nkp46^+$), Myeloid cells($CD45^+$, $CD11b^+$), Neutrophils ($CD45^+$, $CD11b^+$,$F4/80^+$,$Ly6G^+$), Macrophages ($CD45^+$,$CD11b^+$,$F4/80^{hi}$, $Ly6G^+$), cDCs ($CD45^+$,$CD11b^+$,IA/IE^+,$CD11c^+$). n = 6 tumors/group. Data are presented as the mean ± SD. (**C**). Dot plot showing the top 15 GO terms enriched in CD8+ T cells from MDA5 knockout tumor. **(D-G)**. FACS analysis of Perforin+ (**D**), TNFα+ (**E**), GZMB+ (**F**), IFNγ+ (**G**) CD8+ T cells in control or MDA5 KO MC38 tumors. n = 5 tumors/group. Data are presented as mean ± SD. (**H**). Diagram showing the scheme for administration of anti-CD8a, anti-NK1.1/anti-asialo-GM1, anti-Ly6G or an isotype control. (**I-J**). Verification of the efficacy of various immune cell depletion using flow cytometry after treated with corresponding antibodies (n= 3). Statistics were applied using one-way ANOVA (**A-B, D-G**) or a student's t test (**I, J**).

Supplementary Fig. 6 | MDA5-ablation promoted abscopal effect

(A-C) Experimental design for sequential tumor implantation. Mice were initially injected with 5.0×10^5 Hepa1-6 control or Hepa1-6 MDA5 KO cells in the left flank. After 10 days, these mice were subsequently implanted with 2.0×10^6 Hepa1-6 control or MDA5 KO cells in the right flank, as illustrated in (A). Right tumor growth curves were measured at each time point (B). Tumor photographs and tumor weights (C) are also shown. Data are presented as mean ± SEM (B) and mean ± SD (C), with n = 5 mice/group.

Supplementary Fig. 7 | MDA5-null enhances communication between CD8+T cells and DCs

(**A**). Number of significant ligand-receptor pairs from CD8+ Tem to other cells. (**B**). Cell-cell communication analysis (CellChat) showing increased ligand-receptor interactions from CD8+ Tem to cDC2. Only significant interactions are shown. (**C**). Violin plots showing the expression of *Ctla4, Cd28, Itgax, Itgb2, Cd274* in CD8+ Tem cells. **(D)**. WB analysis of NY-EOS-1 OE in HCT15 cells. **(E)**. Tumor photographs for MC38 control or MDA5 knockout tumors in immunocompetent C57BL/6 mice treated with or without FTY720, relative to Fig.4 K-L. **(F)**. Tumor photographs for MC38 control or MDA5 knockout tumors in immunocompetent C57BL/6 mice treated with or without CCR7 antibody, relative to Fig.4 M-N. Statistics were applied using Wilcoxon signed rank test (**C**).

Supplementary Fig. 8 | MDA5 ablation promotes UPR and DAMPs expression

(**A**). Gene set enrichment analysis of RNA-seq data showing top 5 upregulated and downregulated pathways in MDA5 knockout CT26 cells compared with control. (**B**). Gene set enrichment analysis of unfolded protein response signature in MDA5 knockout CT26 cells compared with control. (**C-D**). Gene set enrichment analysis of XBP1 and ATF6 signature in MDA5 knockout MC38 or CT26 cells compared with control. (**E**). Dot plot showing the top 20 GO terms that both enriched in MDA5 knockout MC38 and MDA5 knockout CT26 cells. (**F-G**). Levels of extracellular ATP(**F**) or secreted HMGB1(**G**) in the conditioned medium (CM) of 10^6 control or MDA5 knockout CT26 cells after treated with indicated treatments. n=3 independent experiments. (**H**). Flow cytometry analysis of surface-exposed calreticulin level of CT26 cells after treated with indicated treatments. n=3 independent experiments. (**I-L**). Immunofluorescence staining and quantification of HMGB1(green) and CALR (red) in MC38 and CT26 tumors harvested from immunocompetent (**I, J**) or immunodeficient (**K, L**) mice. Representative images are shown. The image contrast has been edited equally per stain for visibility in the figures, but unedited images were used for analysis. n = 5 tumors/group. mean ± SD are shown. (**M**). Tumor photographs for MC38 control or MDA5 knockout tumors in immunocompetent C57BL/6 mice treated with or without HMGB1-neutralizing antibody and the P2X7 receptor antagonist A438079, relative to Fig.5 F-G. Statistics were applied using one-way ANOVA (**F, G, J, L**).

Supplementary Fig. 9 | DAMPs were correlated to ICD induced DC activation and T cell killing

(**A-C**). A scatter plot showing the correlation between the DAMP signature and ICD signature (**A**), DC activation signature (**B**), CD8 T Effector signature (**C**) in the E-MTAB-12862 dataset. (**D**). Venn diagram showing expressed gene overlap (log_2(fold change [FC]) > 0.6) between two $MDA5^{KO}$ CT26 tumors. These overlapping genes (189) were used as MDA5-null signature. Statistics were applied using Pearson correlation in (**A, B, C**).

Supplementary Fig. 10 | MDA5 ablation sensitizes tumor cell to TNF-induced apoptosis by enhancing ASK1-JNK/P38 pathway

(**A-B**). Representative images illustrating OT-I killing (**A**) and quantitative estimate of live cells after MC38-OVA cell co-cultured with OT-I for 48h (**B**). E: T means effector-to-target. Data are presented as mean ± SD. n = 4 independent repeats. (**C**). Schematic overview of the *in vitro* competition assay. Co-culture of OT-I CD8 T cells and tumor cells were conducted using a series of effector-to-target (E: T) ratios ranging from 1:1 to 0.25:1. (**D**). Representative flow cytometry plots (GFP vs. mCherry) of the competition assay with or without OT-I cells. (**E**). Changes in the proportion of GFP+ and mCherry+ cells following co-culture with OT-I cells at various effector-to-target (E: T) ratios. (**F**). Flow cytometry analysis H-2Kb/H-2Db level of control and MDA5 knockout MC38 cells. n = 3 biologically repeats. (**G**). Flow cytometry analysis the level of SIINFEKL-H2Kb on the surface of control and MC38-MDA5 knockout cells after pulsed with OVA peptide. n = 3 biologically repeats. (**H**). Flow cytometry analysis H-2Kb/H-2Db level of control and MDA5 knockout MC38 cells after treated with TNFα, IFNγ or their combination. n = 3 biologically repeats. (**I**). Illustration of tumor-T cell co-culture experiments conducted in Transwell. (**J-K**). In the Transwell experiment, representative FACS results of apoptosis assay(**J**) and summary of the apoptosis level of control and MDA5 knockout cells in the lower compartment (**K**). **(L)**. Log2 transformed relative cell viability for MDA5 knockout MC38-Luc-OVA cells upon the addition of OT-I T cells, either in the presence or absence of TNFR1 blocking antibody (n = 3 independent experiments). **(M)**. Log2 transformed relative cell viability of MDA5 knockout CT26 cells after treated with IFNγ, TNFα, or their combination (n = 3 independent experiments). **(N-O)**. FACS analysis of TNFR1, IFNGR1, and IFNAR1 cell surface expression on MC38 (N) and CT26 (O) cells, with or without MDA5 knockout (n = 3 independent experiments). **(P)**. WB analysis of MDA5, p-ASK1, ASK1, p-JNK, JNK, p-p38, p38 in Hepa1-6 and HCT15 cells after the indicated treatment. **(Q)**. WB analysis of MDA5, p-JAK2, JAK2 in MC38 and Hepa1-6 cells after the indicated treatment. (**R-S**). The interaction of ASK1 with MDA5 assayed by Co-Immunoprecipitation(**R**) or by Proximity labeling with TurboID (**S**). (**T**)**.** Log2 transformed relative cell viability of MDA5 knockout CT26 cells after treated with IFNγ and TNFα, either

in the presence or absence of GS-4997(n = 3 biologically repeats). Statistics were applied using one-way ANOVA (**B, K**) or two-way ANOVA (**L**, **M, N, O, T**)**.**

Supplementary Fig. 11 | MDA5-null signature predicts better response to ICB

(**A**). GSEA plot showing the enrichment of the MDA5-null signature in responders across multiple human ICB treatment datasets. Abbreviations: NSCLC: Non-Small Cell Lung Cancer; mUC: metastatic Urothelial Cancer; MPM: Malignant Pleural Mesothelioma; CRC: Colorectal Cancer. related to Figure7 G.

Supplementary Table S1

PatientID	Gender	Age	Primary_site	Primary_disease	Response_Status	MSI or MMR Status	Treatment
Patient1	Male	36	Colon	Intramucosal Carcinoma	response	dMMR	Toripalimab
Patient2	Male	44	Colon	Adenocarcinoma	response	dMMR	Toripalimab
Patient3	Male	37	Rectum	Adenocarcinoma	response	MSI-H	Toripalimab+Celebrex
Patient4	Male	53	Colon	Adenocarcinoma	non-response	dMMR	Toripalimab
Patient5	Male	33	Colon	Adenocarcinoma	response	MSI-H	Toripalimab
Patient6	Male	52	Colon	Adenocarcinoma	response	MSI-H	Toripalimab
Patient7	Male	32	Rectum	Adenocarcinoma	response	MSI-H	Sintilimab
Patient8	Female	71	Colon	Intramucosal Carcinoma	response	MSI-H	Toripalimab+Celebrex
Patient9	Male	66	Colon	Adenocarcinoma	non-response	MSI-H	Sintilimab
Patient10	Male	40	Colon	Adenocarcinoma	non-response	MSI-H	Sintilimab
Patient11	Female	54	Colon	Adenocarcinoma	non-response	MSI-H	Toripalimab
Patient12	Male	35	Rectum	Adenocarcinoma	response	MSI-H	Toripalimab+Celebrex
Patient13	Male	52	Rectum	Intramucosal Carcinoma	non-response	MSI-H	Sintilimab
Patient14	Male	45	Rectum	Intramucosal Carcinoma	non-response	MSI-H	Sintilimab
Patient15	Male	56	Rectum	Intramucosal Carcinoma	response	MSI-H	Sintilimab
Patient16	Female	25	Colon	Intramucosal Carcinoma	response	MSI-H	Pembrolizumab+Celebrex
Patient17	Male	30	Colon	Adenocarcinoma	response	MSI-H	Pembrolizumab
Patient18	Male	44	Colon	Intramucosal Carcinoma	response	MSI-H	Toripalimab+Celebrex
Patient19	Male	27	Rectum	Adenocarcinoma	non-response	MSI-H	Sintilimab
Patient20	Male	68	Rectum	Adenocarcinoma	response	MSI-H	Sintilimab + Celebrex
Patient21	Male	39	Rectum	Adenocarcinoma	response	MSI-H	Pembrolizumab
Patient22	Male	59	Colon	Adenocarcinoma	non-response	MSI-H	Nivolumab
Patient23	Male	46	Rectum	Intramucosal Carcinoma	response	MSI-H	Sintilimab
Patient24	Male	32	Rectum	Intramucosal Carcinoma	response	MSI-H	Sintilimab
Patient25	Male	65	Rectum	Adenocarcinoma	response	MSI-H	Sintilimab
Patient26	Male	65	Colon	Adenocarcinoma	response	MSI-H	Pembrolizumab
Patient27	Male	36	Rectum	Adenocarcinoma	non-response	MSI-H	Toripalimab+Celebrex
Patient28	Female	54	Rectum	Adenocarcinoma	non-response	MSI-H	Sintilimab
Patient29	Male	63	Colon	Adenocarcinoma	response	MSI-H	Tislelizumab+Celebrex
Patient30	Female	49	Rectum	Adenocarcinoma	non-response	MSI-H	Tislelizumab

Patient31	Male	45	Colon	Intramucosal Carcinoma	response	MSI-H	Toripalimab+Celebrex
Patient32	Female	68	Colon	Intramucosal Carcinoma	response	MSI-H	Tislelizumab+Oxaliplatin+Capecitabine
Patient33	Female	42	Rectum	Intramucosal Carcinoma	response	MSI-H	Toripalimab
Patient34	Male	49	Colon	Intramucosal Carcinoma	response	MSI-H	Sintilimab +Oxaliplatin+Capecitabine
Patient35	Female	39	Colon	Adenocarcinoma	non-response	MSI-H	Pembrolizumab
Patient36	Male	43	Colon	Adenocarcinoma	response	MSI-H	Pembrolizumab
Patient37	Male	41	Colon	Adenocarcinoma	non-response	MSI-H	Tislelizumab
Patient38	Male	61	Colon	Adenocarcinoma	non-response	MSI-H	Pembrolizumab
Patient39	Male	44	Rectum	Adenocarcinoma	non-response	MSI-H	Sintilimab
Patient40	Female	23	Rectum	Intramucosal Carcinoma	response	MSI-H	Pembrolizumab+Celebrex
Patient41	Female	59	Colon	Adenocarcinoma	response	MSI-H	Tislelizumab
Patient42	Male	36	Rectum	Adenocarcinoma	response	MSI-H	Toripalimab+Celebrex
Patient43	Male	71	Colon	Intramucosal Carcinoma	response	MSI-H	Pembrolizumab
Patient44	Male	60	Rectum	Adenocarcinoma	response	MSI-H	Sintilimab
Patient45	Female	84	Colon	Adenocarcinoma	response	MSI-H	Toripalimab
Patient46	Female	76	Colon	Intramucosal Carcinoma	response	MSI-H	Toripalimab+Celebrex
Patient47	Male	55	Colon	Adenocarcinoma	response	MSI-H	Sintilimab
Patient48	Male	33	Colon	Intramucosal Carcinoma	response	MSI-H	Toripalimab
Patient49	Female	73	Colon	Intramucosal Carcinoma	non-response	MSI-H	Toripalimab
Patient50	Female	55	Rectum	Intramucosal Carcinoma	non-response	MSI-H	Sintilimab
Patient51	Male	61	Colon	Intramucosal Carcinoma	non-response	MSI-H	Sintilimab
Patient52	Male	41	Colon	Adenocarcinoma	non-response	MSI-H	Toripalimab
Patient53	Female	60	Colon	Adenocarcinoma	non-response	MSI-H	Toripalimab
Patient54	Male	27	Rectum	Adenocarcinoma	response	MSI-H	Nivolumab
Patient55	Female	28	Colon	Adenocarcinoma	response	MSI-H	Pembrolizumab
Patient56	Female	26	Colon	Adenocarcinoma	non-response	MSI-H	Toripalimab
Patient57	Female	33	Colon	Adenocarcinoma	response	MSI-H	Pembrolizumab
Patient58	Female	57	Rectum	Adenocarcinoma	non-response	MSI-H	Pembrolizumab+Aspirin
Patient59	Male	63	Colon	Intramucosal Carcinoma	response	dMMR	Toripalimab
Patient60	Male	44	Colon	Mucinous adenocarcinoma	non-response	MSI-H	Pembrolizumab
Patient61	Female	48	Colon	Intramucosal Carcinoma	response	MSI-H	Toripalimab+Celebrex
Patient62	Male	47	Colon	Adenocarcinoma	response	dMMR	Toripalimab

Patient63	Male	23	Rectum	Adenocarcinoma	response	dMMR	Toripalimab
Patient64	Male	65	Colon	Adenocarcinoma	response	MSI-H	Toripalimab+Celebrex
Patient65	Female	57	Colon	Adenocarcinoma	response	dMMR	Toripalimab
Patient66	Female	30	Colon	Adenocarcinoma	non-response	MSI-H	Toripalimab
Patient67	Female	42	Colon	Intramucosal Carcinoma	response	dMMR	Sintilimab
Patient68	Female	45	Colon	Adenocarcinoma	response	dMMR	Toripalimab
Patient69	Male	38	Colon	Adenocarcinoma	response	MSI-H	Toripalimab
Patient70	Female	45	Colon	Intramucosal Carcinoma	response	MSI-H	Toripalimab
Patient71	Female	45	Colon	Intramucosal Carcinoma	non-response	dMMR	Toripalimab
Patient72	Female	67	Colon	Intramucosal Carcinoma	response	dMMR	Toripalimab

Supplementary Table S2

Dataset used in PD1 response analysis

Study	Cancer	Anti Target	Sample Size	Response	Non-Response
GSE99070	Malignant Pleural Mesothelioma	anti-PD1	10	4	6
GSE135222	Non-small Cell Lung Cancer	anti-PDL1	27	8	19
GSE176307	Metastatic Urothelial Cancer	anti-PD1	88	16	72
GSE91061	Melanoma	anti-PD1	51	25	26
PRJEB23709	Metastatic Melanoma	antiPD1/anti-CTLA4	73	46	27
MGSP(phs000452.v3.p1)	Metastatic Melanoma	anti-CTLA4	103	46	57
PMID_27956380	Melanoma	anti-CTLA4	22	6	16
GSE179351	Colorectal Cancer(mss)	anti-CTLA4+ anti-PD1	4	1	3

Supplementary Table **S3**

Primer information

gene	**sequence(5'->3')**
Mice-Actb	Forward :ATCGATCGATGCATGATGC Reverse :TCGATCGATGCATCGATCAT
Mice-Ifih1	Forward :TGCGGAAGTTGGAGTCAAAGCG Reverse :CACCGTCGTAGCGATAAGCAGA
Mice-IFN-α	Forward:GGATGTGACCTTCCTCAGACTC Reverse:ACCTTCTCCTGCGGGAATCCAA
Mice-IFN-β	Forward:GCCTTTGCCATCCAAGAGATGC Reverse:ACACTGTCTGCTGGTGGAGTTC
Mice-IL1β	Forward: TGGACCTTCCAGGATGAGGACA Reverse: GTTCATCTCGGAGCCTGTAGTG

sgRNA Oligos

gene	**sequence(5'->3')**
Mice-sgCtrl	GCGAGGTATTCGGCTCCGCG
Mice-sgIfih1#1	TGGGCCACTTCCATTTGGTA
Mice-sgIfih1#2	TGGGCCACTTCCATTTGGTA
Mice-sgTnfr1#1	GGATCCCGTGCCTGTCAAAG
Mice-sgIfngr1#1	ATTAGAACATTCGTCGGTAC
Human-sgCtrl	GCACTCACATCGCTACATGA
Human-sgIFIH1#1	TGAGCTCAGGGTTCATGTAG
Human-sgIFIH1#2	TCATGAGCGTTCTCAAACGA

shRNA Oligos

gene	**sequence(5'->3')**
Mice-shCtrl	CAACAAGATGAAGAGCACCAA
Mice-shIfih1#1	CCACAGAATCAGACACAAGTT

dsRNA sensor library sgRNA Oligos

gene	**sequence(5'->3')**
Mice-sgCtrl#1	CACCGGCGAGGTATTCGGCTCCGCG
Mice-sgCtrl#2	CACCGGCTTTCACGGAGGTTCGACG
Mice-sgCtrl#3	CACCGGAGGCGGGCTCTTCTATCGT
Mice-sgCtrl#4	CACCGCATACCCGGTGTTTCCTAGC

Mice-sgEif2ak2#1	CACCGCTCCTGCTTTGATCTACCTT
Mice-sgEif2ak2#2	CACCGTTGTTCGTTGGTAACTACAT
Mice-sgEif2ak2#3	CACCGGAAGCTGTTAAAGAGCCCGC
Mice-sgEif2ak2#4	CACCGAAGTATATCAACAGCTAATT
Mice-sgMavs#1	CACCGACTCCTCCAGACCAACTCCG
Mice-sgMavs#2	CACCGGGTCACAACATCCCTGACCA
Mice-sgMavs#3	CACCGGCCACCAGACATCCTCGCGA
Mice-sgMavs#4	CACCGGCCGTCGCGAGGATGTCTGG
Mice-sgNlrp1a#1	CACCGGACATAAGTTTACGGCCCCT
Mice-sgNlrp1a#2	CACCGTGTACGACCCTGAGAAAGCG
Mice-sgNlrp1a#3	CACCGTGTACTGCATAGTAGCTCAG
Mice-sgNlrp1a#4	CACCGAGACCTGCAGCTGAATGACC
Mice-sgNlrp1b#1	CACCGCTAAATGACCTGTGTGACGA
Mice-sgNlrp1b#2	CACCGTGTGATGCCATGATATACCC
Mice-sgNlrp1b#3	CACCGGTGTAGGATGCCACAAATGA
Mice-sgNlrp1b#4	CACCGCCCCAATCACTAATGCCAGT
Mice-sgTLR3#1	CACCGACATTAGATCGAGTTCTGTC
Mice-sgTLR3#2	CACCGGTTCTTCACTTCGCAACGCA
Mice-sgTLR3#3	CACCGCAATTCTTCTTTACGAAAGT
Mice-sgTlr3#4	CACCGTCAGTTGGGCGTTGTTCAAG
Mice-sgTlr9#1	CACCGGGGCCGTAGCATCTTCGCGC
Mice-sgTlr9#2	CACCGCTCGACCGCCAGAGCGAAGA
Mice-sgTlr9#3	CACCGGTCCTTCAATTACCGCAAGA
Mice-sgTlr9#4	CACCGCCGAGCCCTACGCTTGTGTC
Mice-sgTmem173#1	CACCGGTAGAATCATAGCCATACAG
Mice-sgTmem173#2	CACCGGAAGGCCAAACATCCAACTG
Mice-sgTmem173#3	CACCGCGGCAGTTATTTCGAGACTC
Mice-sgTmem173#4	CACCGTACTTGCGGTTGATCTTACC
Mice-sgDdx58#1	CACCGAGAGGAGGTGCAGTACATTC
Mice-sgDdx58#2	CACCGTTGGATGCCCTGTACCATGC
Mice-sgDdx58#3	CACCGTTTGTGAAGCCATCGAAAGT
Mice-sgDdx58#4	CACCGATCCGAATGTTTGATTAATC
Mice-sgIfih1#1	CACCGTGGGCCACTTCCATTTGGTA
Mice-sgIfih1#2	CACCGGGTTATCGTTCTTGTCAATA
Mice-sgIfih1#3	CACCGCGTAGACGACATATTACCAG
Mice-sgIfih1#4	*CACCGACATAACAGCAACATGGGCA*

Gating Strategies for Flow Cytometry

Gating Strategy for Lymphoid cells

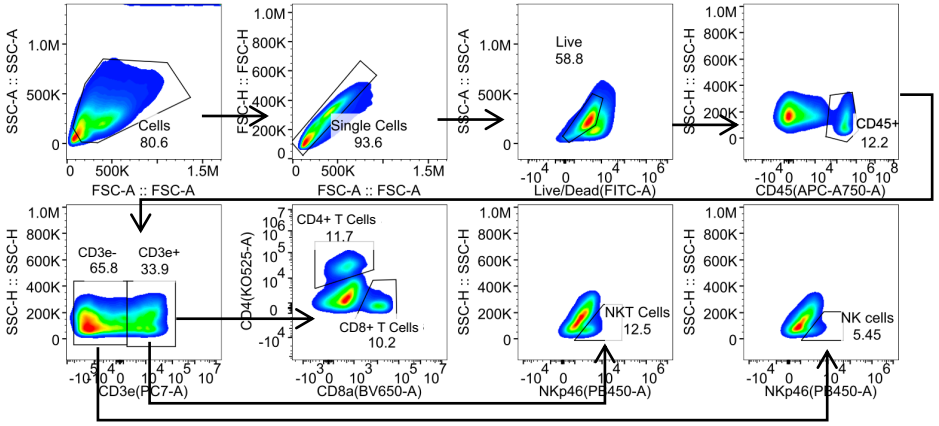

Gating Strategy for Myeloid cells

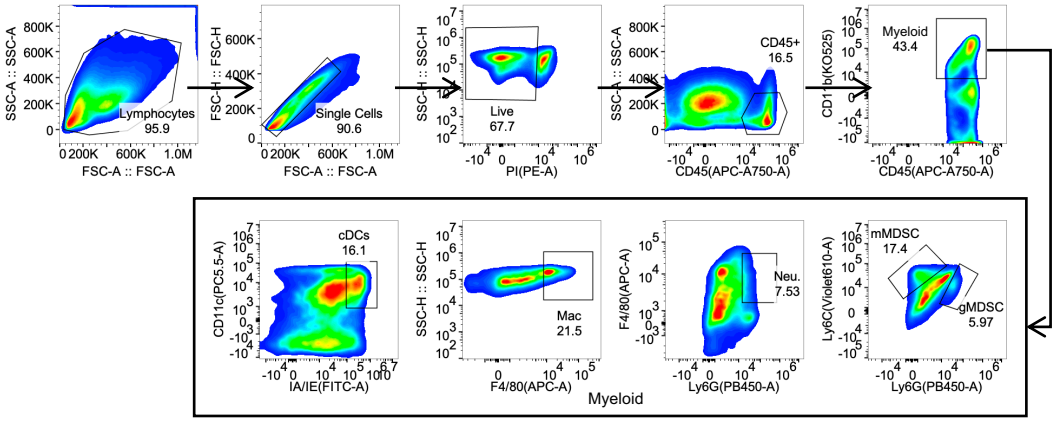

The original uncropped images of western blot

Fig. 1A

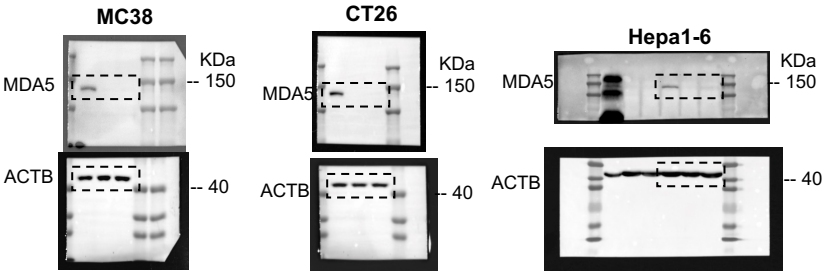

Fig. 6H (MC38 Cell)

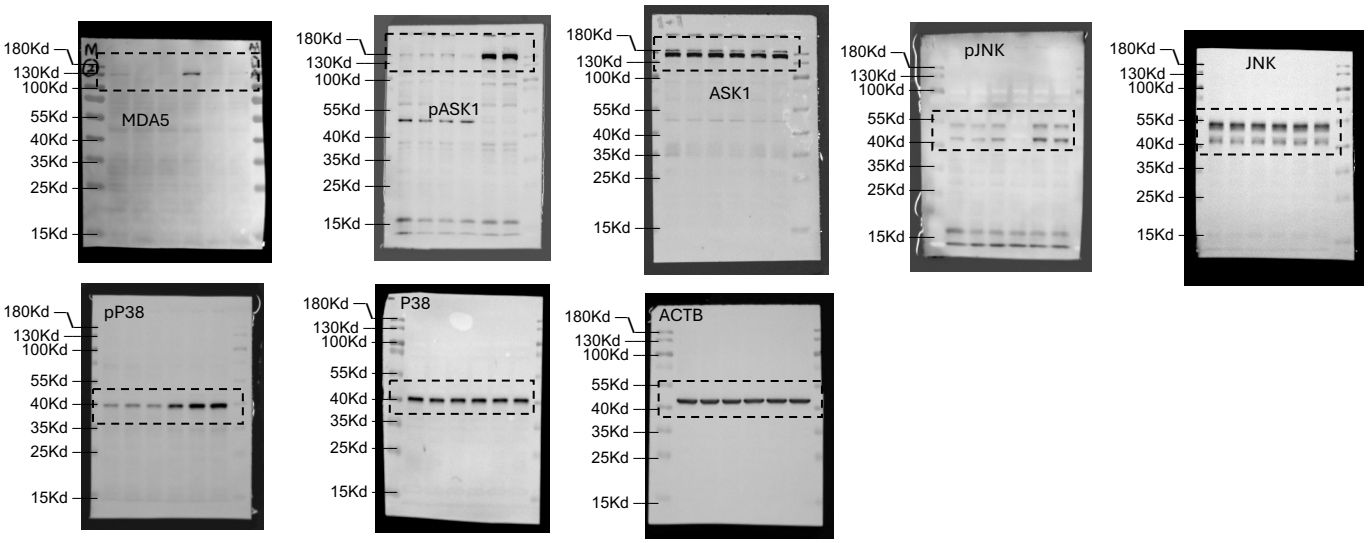

Fig. 6H (DLD1 Cell)

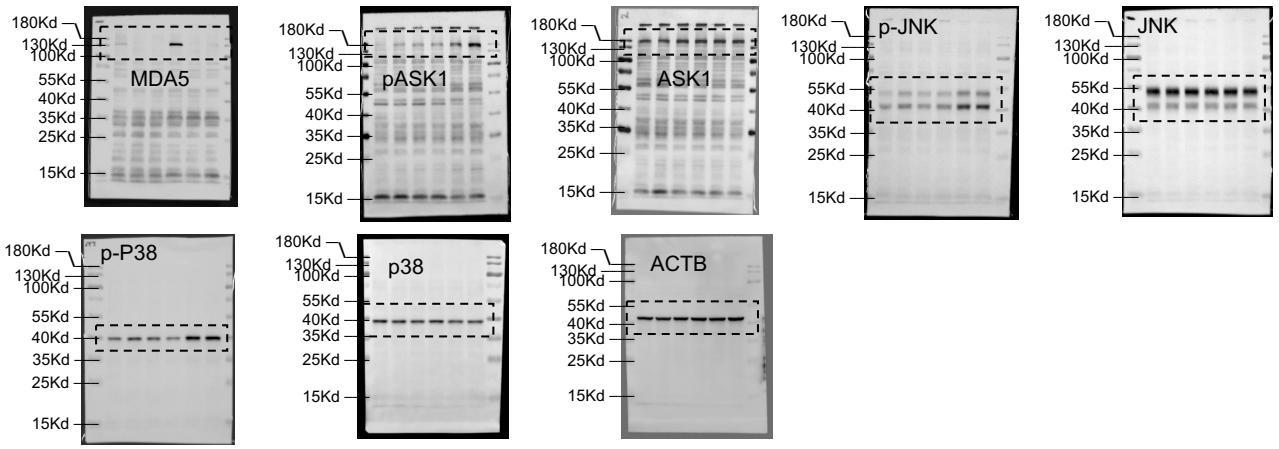

Supplementary Fig. 2B

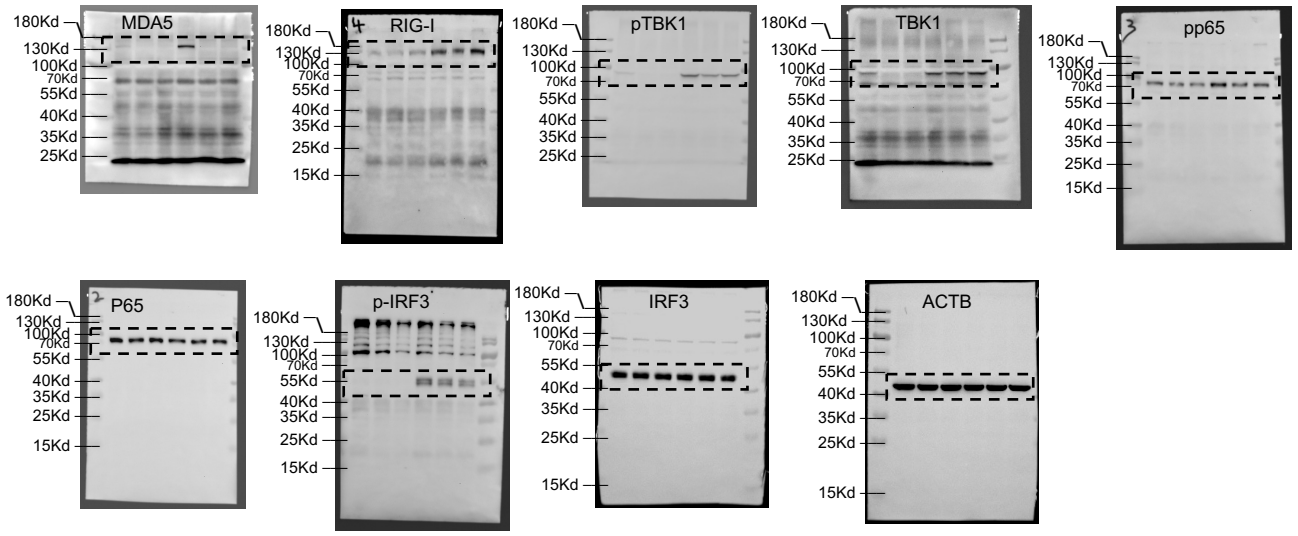

Supplementary Fig. 2C

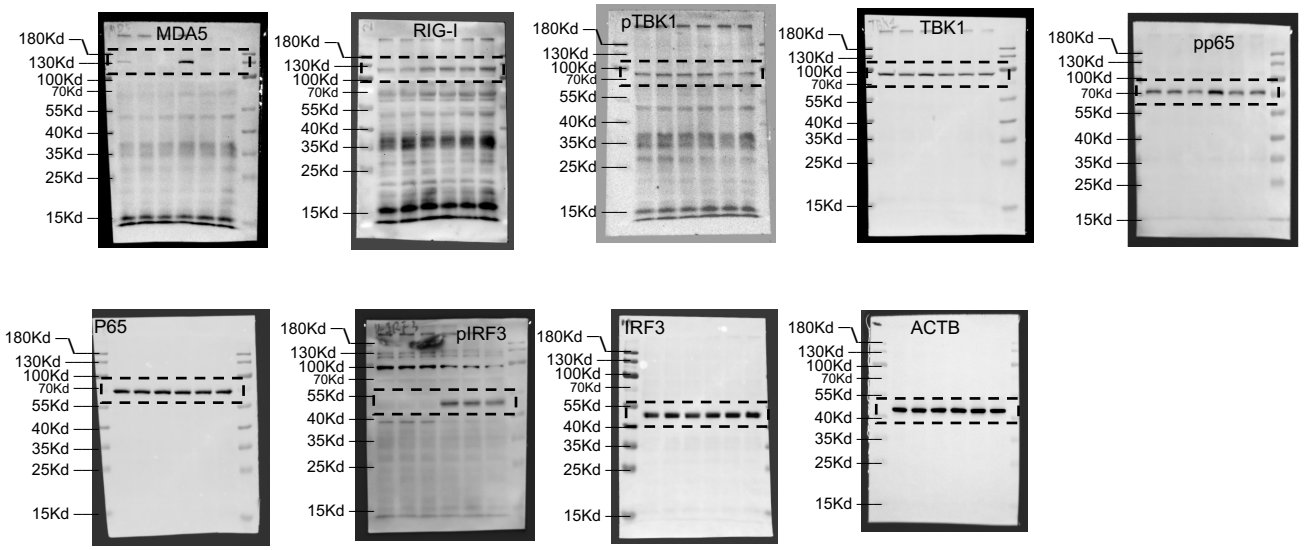

Supplementary Fig. 2D

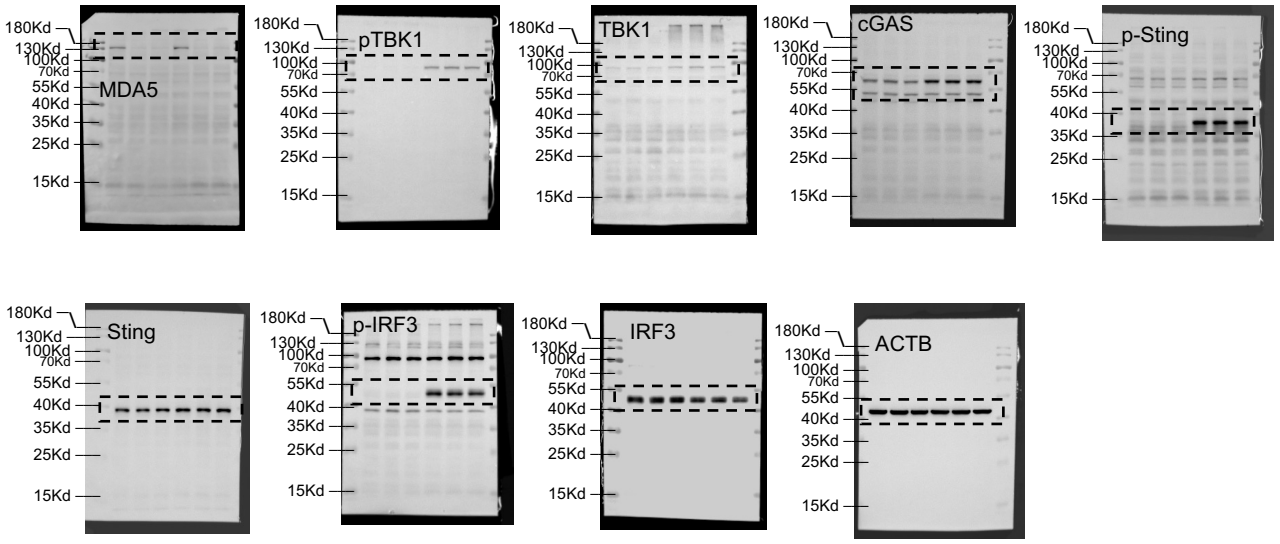

Supplementary Fig. 7D

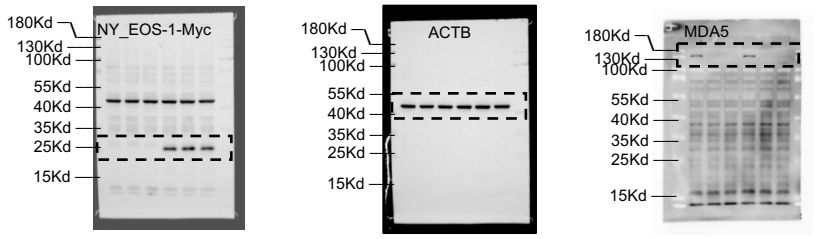

Supplementary Fig. 10P (Hepa 1-6 cell)

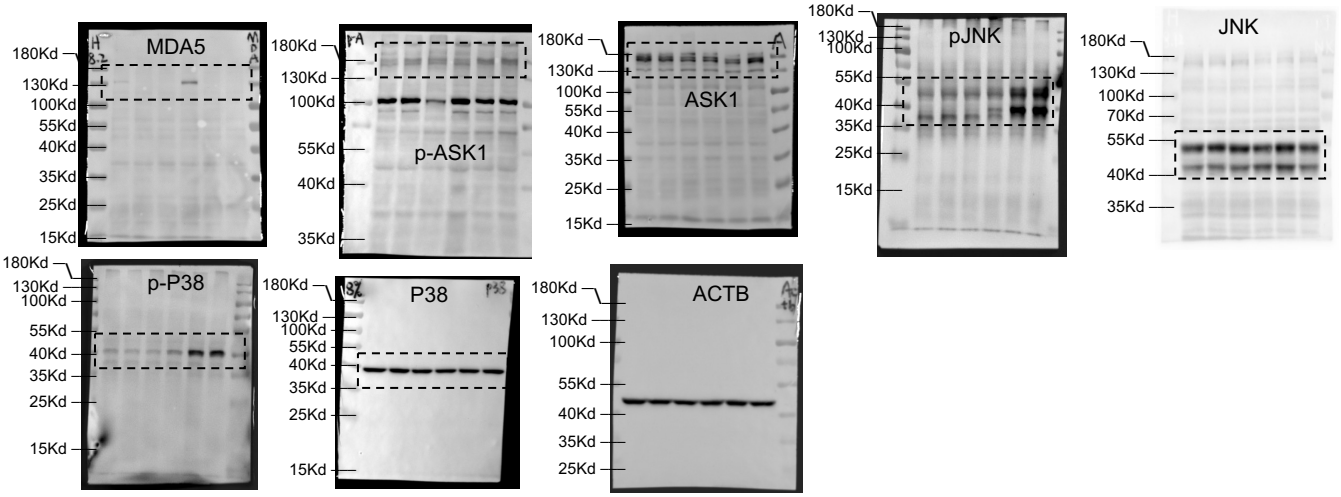

Supplementary Fig. 10P (HCT15 cell)

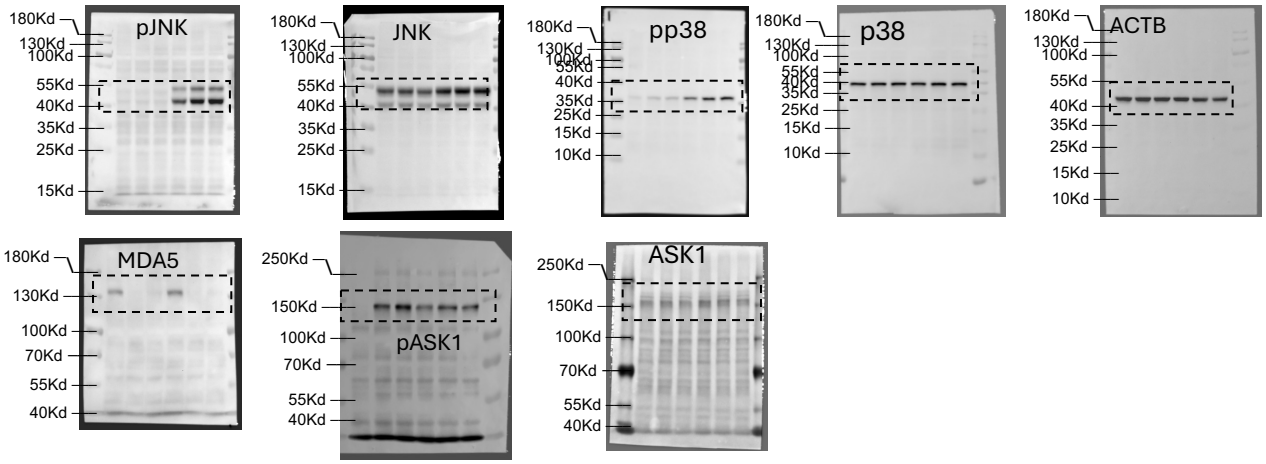

Supplementary Fig. 10Q (HCT15 cell)

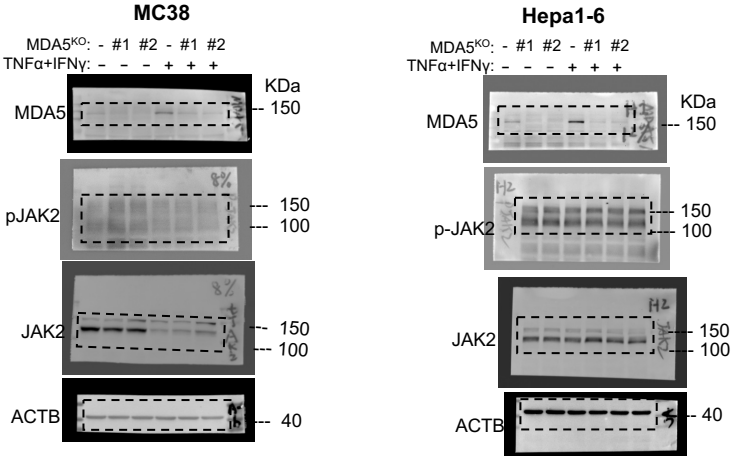

Supplementary Fig. 10R

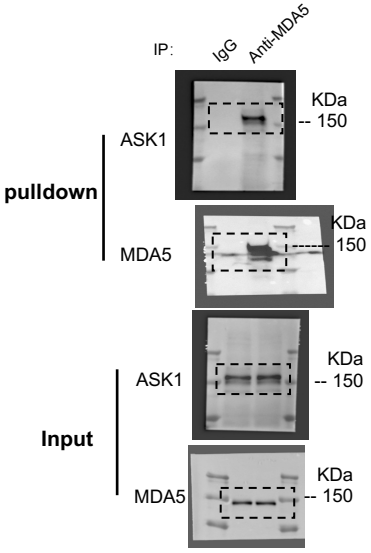

Supplementary Fig. 10S